Inorg. Chem. **1994**, *33*, 1109–1114

Disilylphosphido Complexes $M[P(SiPh_3)_2]_2$, Where M = Zn, Cd, Hg, and Sn: Effective Steric Equivalency of $P(SiPh_3)_2$ and $N(SiMe_3)_2$ Ligands

Michael A. Matchett, Michael Y. Chiang,[†] and William E. Buhro[*]

Department of Chemistry, Washington University, St. Louis, Missouri 63130

Received August 18, 1993[●]

The disilylphosphido complexes $M[P(SiPh_3)_2]_2$, where M = Zn, Cd, Hg, and Sn, are prepared in 50–90% yields and isolated as crystalline solids or powders. Cryoscopic and NMR data indicate that the compounds are monomers in solution. The solid-state structure of $Cd[P(SiPh_3)_2]_2$ reveals a two-coordinate, linear coordination geometry about cadmium and distinctly pyramidal terminal $P(SiPh_3)_2$ ligands. $Cd[P(SiPh_3)_2]_2$ forms unstable adducts with pyridine and PMe_3. NMR titration experiments establish formation constants (K_f's) of 1400(150) and 400(75) M^{-1} for $Cd[P(SiPh_3)_2]_2 \cdot py$ and $Cd[P(SiPh_3)_2]_2 \cdot PMe_3$, respectively. Close similarities between the properties of $M[P(SiPh_3)_2]_2$ complexes and their $M[N(SiMe_3)_2]_2$ analogs establish that the $P(SiPh_3)_2$ ligand, although it contains very bulky $SiPh_3$ substituents, is a steric equivalent to the $N(SiMe_3)_2$ ligand. Preparations of the reagents $LiP(SiPh_3)_2 \cdot 2.0THF$ and $HP(SiPh_3)_2$ are also described. Crystal data for $Cd[P(SiPh_3)_2]_2$: monoclinic, $C2/c$, a = 26.536(5) Å, b = 13.862(2) Å, c = 17.380(3) Å, β = 110.90(1)°, V = 5972(2) Å^3, T = −100 °C, Z = 4.

Introduction

This paper describes a series of homoleptic disilylphosphido complexes containing the bulky $P(SiPh_3)_2$ ligand. Disilylphosphido complexes $M[P(SiR_3)_2]_x$ are heavier congeners of the well-known disilylamido complexes $M[N(SiMe_3)_2]_x$.[1] The first examples from this new class of coordination compounds were recently prepared in our laboratory.[2] The present study was undertaken (1) to extend the initial study, which compared the properties of homologous $M[N(SiMe_3)_2]_x$ and $M[P(SiMe_3)_2]_x$ complexes,[2] and (2) to provide additional disilylphosphido precursors for metallo-organic syntheses of bulk and nanoparticulate phosphide semiconductors.[3,4] We show here that, in terms of structures, stabilities, and Lewis acidities, the new $P(SiPh_3)_2$ complexes more closely resemble the classic $N(SiMe_3)_2$ complexes than do the exact $P(SiMe_3)_2$ homologs.

The earlier comparison of homologous $N(SiMe_3)_2$ and $P(SiMe_3)_2$ complexes found that the phosphido compounds exhibited higher molecularities and higher coordination numbers about both metal and pnictide (N, P) centers.[2] The results confirmed that phosphido ligands are inherently stronger bridge-forming groups than are amido ligands. The stronger bridging tendencies were attributed to normal periodic relationships: the larger size, lower electronegativity, and lower hybridization ability of P as compared to N. In the present study, the bridging tendencies of the phosphido ligands are shown to decrease with the introduction of bulky SiR_3 substituents at P. This structural modification induces $P(SiR_3)_2$ ligands to mimic the classic properties of $N(SiMe_3)_2$ ligands, principally, the ability to stabilize low-coordinate metal centers. Consequently, the $P(SiPh_3)_2$ ligand, although it contains very bulky $SiPh_3$ substituents, is a closer steric equivalent to $N(SiMe_3)_2$ than is $P(SiMe_3)_2$.

We now describe the synthesis and characterization of the stable, homoleptic phosphido complexes $M[P(SiPh_3)_2]_2$, where M = Zn, Cd, Sn, and Hg. We report what is to our knowledge the first X-ray crystal structure of a two-coordinate cadmium compound, $Cd[P(SiPh_3)_2]_2$. We have also characterized the Lewis acidity of $Cd[P(SiPh_3)_2]_2$, as a representative example, by measuring formation constants for the complexation of pyridine and PMe_3. The close comparisons between the behaviors of the bulky disilylphosphido complexes and the corresponding $M[N(SiMe_3)_2]_2$ compounds are discussed.

Experimental Section

General Methods. All reactions were carried out under dry N_2 using standard inert-atmosphere techniques. C, H, and N analyses were performed by Oneida Research Services, Whitesboro, NY. Metal analyses were determined by EDTA titrations.[5] NMR spectra were recorded at a field corresponding to 300 MHz for ^1H on a Varian XL300 instrument. Spectra were referenced to residual protons in benzene-d_6 for ^1H, 1.0 M aqueous LiCl for ^7Li, and external 85% H_3PO_4 for ^{31}P. IR spectra were recorded in KBr on a Mattson FT IR instrument under a N_2 atmosphere. UV–visible absorbance spectra were taken on a Varian Cary 219 instrument.

Starting Materials. CdI_2, $SnCl_2$, and $HgBr_2$ were purchased from Aldrich Chemical Co. and used as received. $ZnCl_2 \cdot xH_2O$ was purchased from Aldrich and dried according to literature procedures.[6] *n*-BuLi was purchased as a 2.5 M solution in hexane from Aldrich and used as received. The $M[N(SiMe_3)_2]_2$ precursors (M = Cd,[7] Hg,[7] Zn,[7] Sn[8]) and $P(SiPh_3)_3$[9] were prepared according to literature procedures.

Solvents. Hexane, pentane, benzene, toluene, and THF were dried over sodium benzophenone ketyl and then distilled. MeOH was dried over $Mg(OMe)_2$ and then distilled. All solvents were stored over type 4A seives under N_2. NMR solvents benzene-d_6, pyridine-d_5, and toluene-d_8 (Aldrich) were sparged with N_2 and stored over type 4A sieves.

Preparation of $LiP(SiPh_3)_2 \cdot 2.0THF$. $P(SiPh_3)_3$ (5.12 g, 6.34 mmol) was dissolved in THF (50 mL) at room temperature and *n*-BuLi (2.80 mL of a 2.5 M hexane solution, 7.0 mmol) was added, resulting in an intense-yellow solution. The solution was stirred at room temperature for 24 h. Hexane (50 mL) was then added, and the mixture was cooled to −20 °C, whereupon colorless crystals of $LiP(SiPh_3)_2 \cdot 2.0THF$ formed. The crystals were collected on a glass frit and washed with hexane (10 mL). Residue hexane was removed by placing the crystals under dynamic

---

[†] Present address: Department of Chemistry, National Sun Yat-Sen University, Kaosiung, Taiwan 804, Republic of China.

[●] Abstract published in *Advance ACS Abstracts*, February 15, 1994.

(1) Lappert, M. F.; Power, P. P.; Sanger, A. R.; Srivastava, R. C. *Metal and Metalloid Amides*; Ellis Horwood: Chichester, England, 1980.

(2) Goel, S. C.; Chiang, M. Y.; Rauscher, D. J.; Buhro, W. E. *J. Am. Chem. Soc.* **1993**, *115*, 160–169.

(3) Goel, S. C.; Chiang, M. Y.; Buhro, W. E. *J. Am. Chem. Soc.* **1990**, *112*, 5636.

(4) Matchett, M. A.; Viano, A. M.; Adolphi, N. L.; Stoddard, R. D.; Buhro, W. E.; Conradi, M. S.; Gibbons, P. C. *Chem. Mater.* **1992**, *4*, 508.

(5) Basset, J.; Denney, R. C.; Jeffery, G. H.; Mendham, J. *Vogel's Textbook of Quantitative Inorganic Analysis*, 4th ed.; Wiley: New York, 1978; pp 324–325.

(6) Pray, A. R. *Inorg. Synth.* **1957**, *5*, 153.

(7) Bürger, H.; Sawodny, W.; Wannagat, U. *J. Organomet. Chem.* **1965**, *3*, 113.

(8) Gynane, M. J. S.; Harris, D. H.; Lappert, M. F.; Power, P. P.; Riviere, P.; Riviere-Baudet, M. *J. Chem. Soc., Dalton Trans.* **1977**, 2004.

(9) Hassler, K. *Monatsh, Chem.* **1982**, *113*, 421.

0020-1669/94/1333-1109$04.50/0

vacuum (10^{-2} Torr) for 15 min. Yield: 3.67 g, 5.52 mmol, 87%. Anal. Calcd for $\mathrm{C_{44}H_{46}LiO_2PSi_2}$: C, 75.38; H, 6.61. Found: C, 74.64; H, 6.47. ^{1}H NMR (δ, benzene-d_6): 7.66 (D, $^3J_{H-H}$ = 7 Hz, 12 H), 7.06 (m, 18 H), 3.42 (m, 8 H, THF), 1.29 (m, 8 H, THF). ^{31}P NMR (ppm, benzene-d_6): −321.2 (s). ^{7}Li NMR (ppm, benzene-d_6): 0.31 (s).

Preparation of $\mathrm{LiP(SiPh_3)_2\cdot}x\mathrm{THF}$. The procedure was conducted as described above for $\mathrm{LiP(SiPh_3)_2\cdot 2.0THF}$, except for the workup. The reaction mixture was stirred for 24 h, and the solvent was removed under vacuum to give a sticky yellow solid. The silane byproduct, *n*-$\mathrm{BuSiPh_3}$, was removed by washing the solid with hexane (4 × 10 mL). The solid was then dried under vacuum for 12 h, leaving $\mathrm{LiP(SiPh_3)_2\cdot}x\mathrm{THF}$ as a light-yellow powder. The amount of the THF solvate (that is, the value of x) was determined by ^{1}H NMR integration; typical values of x were 1.2–2.0. Typical yields were 75–85%. ^{1}H and ^{31}P NMR spectra were consistent with those of $\mathrm{LiP(SiPh_3)_2\cdot 2.0THF}$.

Preparation of $\mathrm{HP(SiPh_3)_2}$. MeOH (0.43 mL, 12.0 mmol) was added to $\mathrm{LiP(SiPh_3)_2\cdot 1.7THF}$ (8.04 g, 12.0 mmol) in toluene (25 mL). The mixture was stirred at room temperature for 2 h and then cooled to −20 °C for 12 h to complete the precipitation of LiOMe. The mixture was then filtered, and the volume of the filtrate was reduced under vacuum to 5 mL. The resulting colorless solution was cooled to −20 °C for 48 h whereupon colorless crystals of $\mathrm{HP(SiPh_3)_2}$ formed. The crystals were collected on a glass frit, washed with 10 mL of hexane, and dried under vacuum. Yield: 4.81 g, 8.70 mmol, 73%. ^{1}H NMR (δ, benzene-d_6): 7.65 (m, 12 H), 7.14 (m, 18 H), 2.06 (d, $^1J_{H-P}$ = 200 Hz, 1 H). ^{31}P NMR (ppm, benzene-d_6): −244.5 (d, $^1J_{P-H}$ = 200 Hz). IR (cm^{-1}, KBr): 3065 m, 3050 m, 3010 w, 3004 w, 2958 w, 2926 w, 2856 w, ν_{P-H} 2274 w, 1483 m, 1426 vs, 1255 w, 1103 vs, 1001 w, 741 m, 735 m, 695 vs, 677 m, 522 vs, 495 s, 482 s.

Preparation of $\mathrm{Zn[P(SiPh_3)_2]_2}$. Solutions of $\mathrm{Zn[N(SiMe_3)_2]_2}$ (1.50 g, 3.89 mmol) in warm toluene (20 mL) and $\mathrm{LiP(SiPh_3)_2\cdot 1.2THF}$ (5.43 g, 8.44 mmol) in warm toluene (20 mL) were combined and stirred. After a few minutes $\mathrm{Zn[P(SiPh_3)_2]_2}$ began to precipitate as a colorless microcrystalline powder. The supernatant was decanted after 12 h, and the crystals were washed with hexane and dried under vacuum, leaving the product as a light-yellow solid. Yield: 2.27 g, 1.97 mmol, 50%. Anal. Calcd for $\mathrm{C_{72}H_{60}P_2Si_4Zn}$: C, 74.22; H, 5.20; Zn, 5.63. Found: C, 75.69; H, 5.76; Zn, 5.21. ^{1}H NMR (δ, benzene-d_6): 7.48 (d, $^3J_{H-H}$ = 6 Hz, 24 H), 7.07 (t, $^3J_{H-H}$ = 6 Hz, 12 H), 6.98 (pseudo t, ^3J = 7 Hz, 24 H). ^{31}P NMR (ppm, benzene-d_6): −245.4 (s). ^{31}P NMR (ppm, pyridine): −298.7 (s), −310.7 (s, minor unassigned resonance), −313.8 (s, minor unassigned resonance). IR (cm^{-1}, KBr): 3066 m, 3048 m, 3017 w, 3010 w, 1483 w, 1427 s, 1104 s, 737 w, 697 vs, 677 m, 518 vs, 495 m.

Preparation of $\mathrm{Cd[P(SiPh_3)_2]_2}$. Method A. $\mathrm{Cd[N(SiMe_3)_2]_2}$ (4.00 g, 9.24 mmol) was dissolved in toluene (20 mL), and the mixture was added to a solution of $\mathrm{LiP(SiPh_3)_2\cdot 1.2THF}$ (12.9 g, 20.1 mmol) in toluene (20 mL). The light yellow solution was allowed to stand overnight at room temperature and then cooled to −20 °C for several hours, whereupon $\mathrm{Cd[P(SiPh_3)_2]_2}$ precipitated as a colorless microcrystalline powder. The supernatant was decanted, and the powder was washed with pentane (10 mL) and dried under vacuum. Yield: 10.5 g, 8.78 mmol, 95%. Anal. Calcd for $\mathrm{C_{72}H_{60}CdP_2Si_4}$: C, 71.43; H, 5.00; Cd, 9.27. Found: C, 71.55; H, 5.12; Cd, 9.07. ^{1}H NMR (δ, toluene-d_8): 7.42 (d, $^3J_{H-H}$ = 8 Hz, 24 H), 7.10 (t, $^3J_{H-H}$ = 8 Hz, 12 H), 6.98 (pseudo t, $^3J_{H-H}$ = 8 Hz, 24 H). ^{31}P NMR (ppm, toluene-d_8): −237.4 (s, $^1J_{P-Cd}$ = 344 Hz, 25% intensity satellites). ^{31}P NMR (ppm, pyridine-d_5): −289.7 (s, $^1J_{P-Cd}$ = 774 Hz, 25% intensity satellites). IR (cm^{-1}, KBr): 3066 m, 3044 m, 3002 w, 1465 w, 1427 s, 1269 w, 1102 s, 737 m, 722 m, 698 vs, 678 w, 528 vs, 483 s.

$\mathrm{Cd[P(SiPh_3)_2]_2}$ was recrystallized from warm toluene. Crystals left standing in air for 48 h showed no signs of decomposition either by visual inspection or by ^{31}P NMR.

Method B. $\mathrm{Cd[N(SiMe_3)_2]_2}$ (2.20 g, 5.08 mmol) was dissolved in toluene (30 mL), and the mixture was added to a solution of $\mathrm{HP(SiPh_3)_2}$ (5.60 g, 10.20 mmol) in toluene (30 mL). The reaction mixture was stirred for 6 h at room temperature, and then the solvent and the byproduct $\mathrm{HN(SiMe_3)_2}$ were removed under vacuum. The resulting crude solid was dissolved in a minimum amount of toluene (10 mL) with warming, and the solution was slowly cooled to 10 °C. Colorless crystals of $\mathrm{Cd[P(SiPh_3)_2]_2}$ were deposited. Yield: 5.57 g, 4.60 mmol, 90%. The Cd analysis and the ^{1}H NMR, ^{31}P NMR, and IR spectra matched those of $\mathrm{Cd[P(SiPh_3)_2]_2}$ obtained by method A.

Preparation of $\mathrm{Hg[P(SiPh_3)_2]_2}$. Solutions of $\mathrm{Hg[N(SiMe_3)_2]_2}$ (0.95 g, 1.82 mmol) in toluene (20 mL) and $\mathrm{LiP(SiPh_3)_2\cdot 1.2THF}$ (2.54 g, 3.95 mmol) in toluene (20 mL) were combined and held at room temperature for 12 h, whereupon colorless crystals of $\mathrm{Hg[P(SiPh_3)_2]_2}$ precipitated from solution. The supernatant was decanted, and the crystals were washed with hexane (5 mL) and dried under vacuum. The volume of the supernatant was reduced and stored at −20 °C, giving a second crop of crystals that was treated as the first. Yield: 2.15 g, 1.67 mmol, 91%. Anal. Calcd for $\mathrm{C_{72}H_{60}HgP_2Si_4}$: C, 66.51; H, 4.66. Found: C, 66.74; H, 4.99. ^{1}H NMR (δ, benzene-d_6): 7.46 (d, $^3J_{H-H}$ = 6 Hz, 24 H), 7.10 (t, $^3J_{H-H}$ = 6 Hz, 24 H), 6.97 (pseudo t, ^3J = 7 Hz, 24 H). ^{31}P NMR (ppm, toluene): −182.7 (s). ^{31}P NMR (ppm, pyridine): −183.0 (s). ($\mathrm{Hg[P(SiPh_3)_2]_2}$ is very sparingly soluble in pyridine.) IR (cm^{-1}, KBr): 3065 w, 3050 w, 3018 vw, 3012 vw, 1483 m, 1426 vs, 1103 vs, 741 m, 736 m, 695 vs, 677 m, 523 vs, 495 s, 482 s.

Table 1. Crystallographic Data for $\mathrm{Cd[P(SiPh_3)_2]_2}$

chem formula	$\mathrm{C_{72}H_{60}P_2Si_4Cd}$	space group	$C2/c$
a (Å)	26.536(5)	T (°C)	−100
b (Å)	13.862(2)	λ (Å)	0.710 73
c (Å)	17.380(3)	ρ_{calcd} (g/cm^3)	1.348
β (deg)	110.90(1)	μ (cm^{-1})	5.36
V (Å^3)	5972(2)	$R(F_o)^a$	0.0241
Z	4	$R_w(F_o)^b$	0.0311
fw	1211.9		

[a] $R(F_o) = \sum||(F_o)| - |F_c)||/\sum|(F_o)|$. [b] $R_w(F_o) = (\sum w||(F_o)| - |(F_c)||^2/\sum w|(F_o)|^2)^{1/2}$, where $w = [\sigma^2(F_o) + 0.0002(F_o)^2]^{-1}$.

Crystals of $\mathrm{Hg[P(SiPh_3)_2]_2}$ left standing in air for 48 h showed no signs of decomposition either by visual inspection or by ^{31}P NMR.

Preparation of $\mathrm{Sn[P(SiPh_3)_2]_2}$. Solutions of $\mathrm{Sn[N(SiMe_3)_2]_2}$ (0.40 g, 0.91 mmol) in benzene (25 mL) and $\mathrm{LiP(SiPh_3)_2\cdot 1.2THF}$ (1.17 g, 1.82 mmol) in benzene (25 mL) were combined to give a dark red solution. The reaction mixture was stirred at room temperature for 4 h, and then the solvent was removed under vacuum leaving a red solid. The solid was washed with hexane (4 × 25 mL) to remove the $\mathrm{LiN(SiMe_3)_2}$ byproduct. The resulting red powder was pure $\mathrm{Sn[P(SiPh_3)_2]_2}$. Yield: 0.60 g, 0.49 mmol, 54%. Anal. Calcd for $\mathrm{C_{72}H_{60}P_2Si_4Sn}$: C, 70.99; H, 4.93. Found: C, 70.56; H, 4.56. ^{1}H NMR (δ, benzene-d_6): 7.64 (d, $^3J_{H-H}$ = 7 Hz, 24 H), 7.24 (t, $^3J_{H-H}$ = 7 Hz, 12 H), 7.16 (pseudo t, ^3J = 7 Hz, 24 H). ^{31}P NMR (ppm, THF): −175.4 (s, $^1J_{P-Sn}$ = 1323 Hz, 14% intensity satellites). IR (cm^{-1}, KBr): 3066 w, 3048, w, 3019 vw, 3014 vw, 3006 w, 1483 w, 1427 s, 1260 vw, 1103 s, 1066 w, 1044 vw, 1039 vw, 1028 w, 997 w, 735 m, 696 vs, 677 m, 524 vs, 496 s, 482 s. Cryoscopic molecular weight determinations used benzene solutions of $\{\mathrm{Sn[P(SiPh_3)_2]_2}\}_n$ (two separate solutions, three determinations for each, mean concentration = 9.0 mg/mL): found n = 0.93(5).

Crystal Structure Determination for $\mathrm{Cd[P(SiPh_3)_2]_2}$. A suitable crystal (0.40 × 0.55 × 0.60 mm) was obtained by recrystallization from benzene and sealed in a glass capillary. Low-temperature (−100 °C) data collection was carried out with ω scanning mode using monochromated Mo Kα radiation on a Nicolet P3 diffractometer. A monoclinic unit cell and orientation were determined on the basis of the setting angles of 15 centered reflections. A variable scan rate of 4.88–14.65 °/min in ω was used throughout the data collection (3.5° < 2θ < 50.0°). Three check reflections were measured every 100 reflections, and no significant variation in intensities was found. A total of 11 327 reflections were collected. Lorentz, polarization, and empirical absorption corrections were applied to the data set in which 4349 unique reflections with $I > 6\sigma(I)$ were retained and used in the subsequent structure analysis.

Solution and refinement were completed using the Siemens SHELXTL PLUS program package (on a Microvax II). The space-group assignment, $C2/c$, was based on statistical data from direct-method output and was subsequently confirmed by successful refinement and convergence. The structure was solved by direct methods. Hydrogens were placed in unrefined, calculated positions, and assigned a common, refined, thermal parameter. Refinement was carried out by use of the full-matrix least-squares method. Crystallographic data and atomic positional parameters are given in Tables 1 and 2, respectively.

Determination of Formation Constants for $\mathrm{Cd[P(SiPh_3)_2]_2\cdot L}$ Adducts. Stock solutions of $\mathrm{Cd[P(SiPh_3)_2]_2}$ in toluene were prepared (0.0033 M). Aliquots (1.0 mL) of stock solution were then transferred to 5-mm NMR tubes, which were capped with rubber septa. The ligands (pyridine, THF, $\mathrm{PMe_3}$) were subsequently added to the tubes by a microliter syringe. Amounts of ligands were added such that the molar ratios of ligand (L) to $\mathrm{Cd[P(SiPh_3)_2]_2}$ ranged L:$\mathrm{Cd[P(SiPh_3)_2]_2}$ = 0.10–16. Pyridine, $\mathrm{PMe_3}$, and THF were transferred as benzene solutions (0.052–0.056 M). ^{31}P NMR spectra were recorded for each sample, and the chemical shifts (δ_P) of the $\mathrm{P(SiPh_3)_2}$ resonance as a function of the total (free plus complexed) ligand and total (free plus complexed) $\mathrm{Cd[P(SiPh_3)_2]_2}$

Table 2. Atomic Positional Parameters (×10^5) and U(eq) (Å^2 × 10^4) for $Cd[P(SiPh_3)_2]_2$

atom	x	y	z	U(eq)^a
Cd	25 000	25 000	0	227(1)
P	32 213(2)	21 223(4)	−5 017(3)	189(2)
Si(1)	38 987(2)	17 870(4)	6 854(3)	198(2)
Si(2)	33 583(2)	36 089(4)	−8 896(3)	179(2)
C(1)	45 415(8)	16 353(15)	4 789(13)	229(7)
C(2)	45 287(9)	13 319(16)	−2 885(13)	276(8)
C(3)	49 972(9)	11 449(18)	−4 428(14)	349(9)
C(4)	54 902(9)	12 572(18)	1 743(15)	379(9)
C(5)	55 166(9)	15 588(19)	9 447(16)	403(9)
C(6)	50 474(9)	17 457(18)	10 976(14)	326(8)
C(7)	37 258(9)	5 971(16)	10 505(13)	254(8)
C(8)	32 841(9)	397(16)	6 115(14)	300(8)
C(9)	31 780(11)	−8 325(18)	9 104(15)	416(10)
C(10)	35 097(12)	−11 587(18)	16 607(16)	474(11)
C(11)	39 510(13)	−6 274(2)	21 105(16)	573(12)
C(12)	40 586(11)	2 410(19)	18 109(15)	446(10)
C(13)	39 630(8)	26 901(15)	15 212(12)	227(7)
C(14)	36 052(9)	26 383(17)	19 453(13)	303(8)
C(15)	35 894(11)	33 587(18)	24 856(15)	401(10)
C(16)	39 348(11)	41 368(18)	26 253(14)	390(10)
C(17)	42 972(9)	41 924(17)	22 278(14)	342(9)
C(18)	43 128(8)	34 739(16)	16 802(13)	272(8)
C(19)	41 094(8)	36 153(14)	−10 556(12)	209(7)
C(20)	40 630(9)	32 998(16)	−17 869(13)	271(8)
C(21)	45 579(9)	32 465(19)	−18 816(15)	372(9)
C(22)	50 216(9)	35 159(19)	−12 422(15)	381(9)
C(23)	49 890(9)	38 309(18)	−5 170(15)	370(9)
C(24)	44 916(8)	38 843(16)	−4 219(13)	284(8)
C(25)	27 972(8)	37 596(16)	−19 160(12)	233(7)
C(26)	25 179(8)	46 207(19)	−21 646(14)	359(9)
C(27)	21 284(11)	47 189(23)	−29 454(17)	503(11)
C(28)	20 143(10)	39 628(25)	−34 905(15)	503(11)
C(29)	22 803(10)	31 019(22)	−32 584(14)	436(10)
C(30)	26 621(9)	29 948(18)	−24 801(13)	314(8)
C(31)	33 549(8)	46 781(15)	−2 236(12)	206(7)
C(32)	31 863(8)	46 627(16)	4 504(12)	245(7)
C(33)	31 721(9)	54 866(18)	8 854(14)	334(9)
C(34)	33 284(10)	63 587(18)	6 637(15)	383(9)
C(35)	35 092(9)	63 983(17)	106(14)	354(9)
C(36)	35 192(9)	55 730(16)	−4 246(13)	279(8)

^{a} U(eq) defined as one-third of the trace of the orthogonalized $\mathbf{U}_{ij}$ tensor.

Table 3. ^{31}P NMR Chemical Shift (δ_P) of $Cd[P(SiPh_3)_2]_2$ in the Presence of Pyridine

$[C_5H_5N]_{tot.}$ (M)	$[Cd[P(SiPh_3)_2]_2]_{tot.}$ (M)	obsd δ_P (ppm)
0	0.003 30(7)	−237.9
0.001 20(5)	0.003 20(6)	−248.1
0.002 40(7)	0.003 10(6)	−252.3
0.004 50(8)	0.003 00(6)	−261.8
0.006 50(9)	0.002 90(6)	−264.9
0.008 30(9)	0.002 80(6)	−265.2
0.012 0(1)	0.002 50(5)	−267.0
0.014 0(1)	0.002 40(5)	−267.2
0.017 0(1)	0.002 20(4)	−267.4
0.022 0(1)	0.001 80(4)	−267.2

Table 4. ^{31}P NMR Chemical Shift (δ_P) of $Cd[P(SiPh_3)_2]_2$ in the Presence of PMe_3

$[PMe_3]_{tot.}$ (M)	$[Cd[P(SiPh_3)_2]_2]_{tot.}$ (M)	obsd δ_P (ppm)
0	0.003 30(7)	−237.9
0.001 00(4)	0.003 20(6)	−239.1
0.002 00(8)	0.003 15(6)	−239.9
0.002 90(9)	0.003 10(6)	−240.8
0.004 70(11)	0.003 00(6)	−242.1
0.006 40(13)	0.002 90(6)	−242.6
0.008 30(14)	0.002 80(6)	−243.1
0.011 70(2)	0.002 60(5)	−244.1
0.016 00(2)	0.002 30(5)	−243.8
0.022 1(2)	0.001 90(4)	−244.9
0.026 5(2)	0.001 60(4)	−245.2

concentrations were compiled. The data are given in Tables 3 (for pyridine) and 4 (for PMe_3). Observed δ_P's did not vary with added THF.

An equation deriving the adduct formation constants from the total ligand and $Cd[P(SiPh_3)_2]_2$ concentrations and the observed chemical shifts was taken from the literature (see Results).[10] The formation constants and limiting adduct chemical shifts were obtained by least-squares fitting of calculated chemical shifts to observed chemical shifts. The data and fits were plotted as δ_P vs L:$Cd[P(SiPh_3)_2]_2$ ratio (see Figure 3). Errors were propagated by standard methods.[11] The largest source of error contributing to the determination of formation constants was in the volumetric measurements; thus, error bars were assigned in the plots to the L:$Cd[P(SiPh_3)_2]_2$ values. The values of the resulting formation constants are recorded in the Results. Limiting adduct chemical shifts of −268.8 ppm for $Cd[P(SiPh_3)_2]_2{\cdot}py$ and −245.3 ppm for $Cd[P(SiPh_3)_2]_2{\cdot}PMe_3$ were determined.

Results

Synthesis and Properties. The $P(SiPh_3)_2$ ligands were introduced into the new disilylphosphido complexes with the reagents $LiP(SiPh_3)_2{\cdot}x$THF or $HP(SiPh_3)_2$. To our knowledge, these reagents have not appeared in the chemical literature. $LiP(SiPh_3)_2{\cdot}x$THF was prepared by lithiation of $P(SiPh_3)_3$[9] with *n*-BuLi by adapting the method of Fritz and Hölderich for $LiP(SiMe_3)_2{\cdot}x$THF.[12] The disolvate $LiP(SiPh_3)_2{\cdot}2.0$THF was obtained by recrystallization from THF/hexane and was prone to the partial loss of THF under vacuum. When isolated as a powder, $LiP(SiMe_3)_2{\cdot}x$THF contained variable amounts of THF (x = 1.2–2.0). $HP(SiPh_3)_2$ was prepared by methanolysis of $LiP(SiMe_3)_2{\cdot}x$THF. A direct preparation of $HP(SiPh_3)_2$ by methanolysis of $P(SiPh_3)_3$ was not successful because mixtures of $HP(SiPh_3)_2$, $H_2P(SiPh_3)$, and PH_3 were generated and were not easily separable. Consequently, $LiP(SiPh_3)_2{\cdot}x$THF and $HP(SiPh_3)_2$ were conveniently obtained from $P(SiPh_3)_3$ in one and two steps, respectively.

The bulky disilylphosphido complexes $M[P(SiPh_3)_2]_2$, M = Zn, Cd, Hg, and Sn, were prepared in 50–90% yields according to eq 1 and were characterized by elemental analyses (C, H, N, and M except Sn) and IR, ^1H, and ^{31}P NMR spectroscopy. All were isolated as colorless crystalline solids except for $Sn[P(SiPh_3)_2]_2$, which was obtained as a red powder. All were slightly to moderately soluble in toluene and benzene and insoluble in hexane. The eq 1 synthesis using the disilylamido precursors and $LiP(SiPh_3)_2{\cdot}x$THF is analogous to the synthesis of $Ge[CH(SiMe_3)_2]_2$ by Lappert and co-workers, in which the precursors $Ge[N(SiMe_3)_2]_2$ and $LiCH(SiMe_3)_2$ were employed.[13] The separation of the $LiN(SiMe_3)_2$ byproduct in eq 1 relied on its greater solubility than the $M[P(SiPh_3)_2]_2$ products. Thus, the generally low solubility of the $M[P(SiPh_3)_2]_2$ complexes (except for $Sn[P(SiPh_3)_2]_2$) facilitated their isolation from eq 1.

$$M[N(SiMe_3)_2]_2 + 2LiP(SiPh_3)_2 \rightarrow M[P(SiPh_3)_2]_2 + 2LiN(SiMe_3)_2 \quad (1)$$

$$M = Zn, Cd, Hg, Sn$$

Alternatively, $Cd[P(SiPh_3)_2]_2$ was prepared from the disilylamido precursor and $HP(SiPh_3)_2$ as shown in eq 2. The analogous synthesis using disilylamido precursors and $HP(SiMe_3)_2$ was used previously for preparing the corresponding $\{M[P(SiMe_3)_2]_2\}_2$

$$Cd[N(SiMe_3)_2]_2 + 2HP(SiPh_3)_2 \rightarrow Cd[P(SiPh_3)_2]_2 + 2HN(SiMe_3)_2 \quad (2)$$

---

(10) Roach, E. T.; Handy, P. R.; Popov, A. I. *Inorg. Nucl. Chem. Lett.* **1973**, *9*, 359.

(11) Bevington, P. R. *Data Reduction and Error Analysis for the Physical Sciences*; McGraw-Hill: New York, 1969.

(12) Fritz, G.; Holderich, W. *Z. Anorg. Allg. Chem.* **1976**, *422*, 104.

(13) Davidson, P. J.; Harris, D. H.; Lappert, M. F. *J. Chem. Soc., Dalton Trans.* **1976**, 2268.

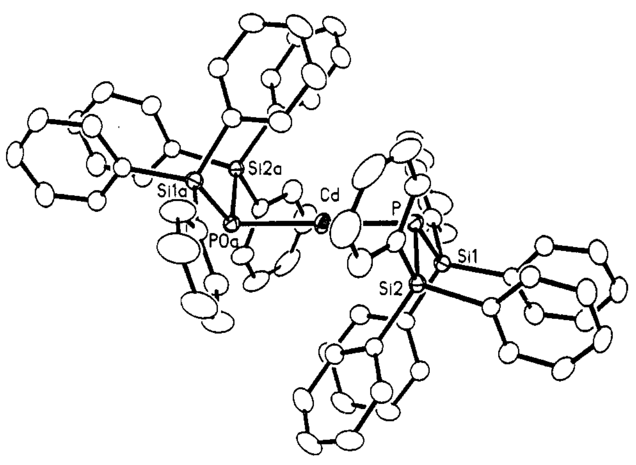

Figure 1. Thermal ellipsoid plot of $\mathrm{Cd[P(SiPh_3)_2]_2}$. Selected bond lengths (Å): Cd–P, 2.427(1); P–Si, 2.249(1). Selected angles (deg): P–Cd–PA, 180.0(1); Cd–P–Si(1), 100.9(1); Cd–P–Si(2), 98.2(1); Si(1)–P–Si(2), 107.7(1).

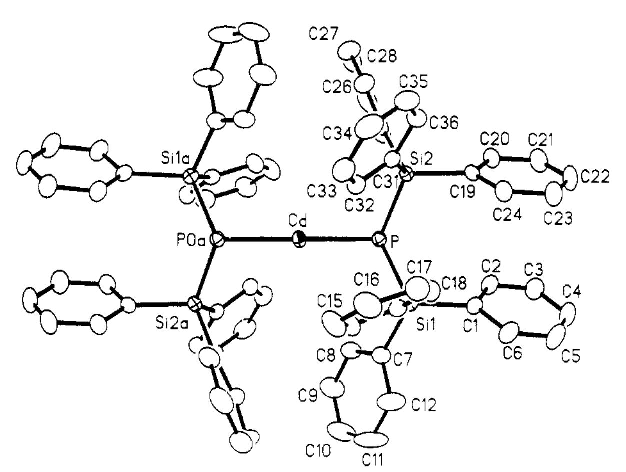

Figure 2. Thermal ellipsoid plot of $\mathrm{Cd[P(SiPh_3)_2]_2}$ showing the atom-numbering scheme.

complexes.[2] However, eq 1 is preferred over eq 2 here because of the extra step required to obtain $\mathrm{HP(SiPh_3)_2}$ (see above). Equation 2 was not extended to the other $\mathrm{M[P(SiPh_3)_2]_2}$ examples.

The $\mathrm{M[P(SiPh_3)_2]_2}$ compounds exhibited considerably higher thermal and air stabilities than the $\mathrm{\{M[P(SiMe_3)_2]_2\}_2}$ analogs. The $\mathrm{M[P(SiPh_3)_2]_2}$ compounds showed no signs of decomposition in 90 °C toluene solutions after 24 h. Extensive decomposition of the corresponding $\mathrm{\{M[P(SiMe_3)_2]_2\}_2}$ compounds occurred under similar conditions.[2] Crystalline $\mathrm{Cd[P(SiPh_3)_2]_2}$ and $\mathrm{Hg[P(SiPh_3)_2]_2}$ showed no signs of decomposition after 48 h of air exposure. The $\mathrm{\{M[P(SiMe_3)_2]_2\}_2}$ compounds spontaneously ignited upon air contact.[2] The $\mathrm{M[P(SiPh_3)_2]_2}$ compounds possessed thermal stabilities comparable to the analogous $\mathrm{M[N(SiMe_3)_2]_2}$ compounds and greater air stabilities. Thus, the $\mathrm{M[P(SiPh_3)_2]_2}$ derivatives were quite robust.

Structure. The $\mathrm{M[P(SiPh_3)_2]_2}$ compounds adopted monomeric, two-coordinate structures in solution and in the solid-state similar to the structures adopted by the corresponding $\mathrm{M[N(SiMe_3)_2]_2}$ compounds.[1] The structures differed from those adopted by the $\mathrm{\{M[P(SiMe_3)_2]_2\}_2}$ compounds, which were dimeric and possessed both bridging and terminal $\mathrm{P(SiMe_3)_2}$ ligands (except for $\mathrm{Hg[P(SiMe_3)_2]_2}$).[2] The data supporting monomeric structures for the $\mathrm{M[P(SiPh_3)_2]_2}$ compounds are presented below.

Solution-phase data were collected by cryoscopic molecular-weight measurement and by ^{31}P NMR. Only $\mathrm{Sn[P(SiPh_3)_2]_2}$ possessed sufficient solubility for cryoscopy in benzene; a molecularity of 0.93(5) was determined. Each of the $\mathrm{M[P(SiPh_3)_2]_2}$ compounds exhibited a single resonance in the ^{31}P NMR spectrum, consistent with monomeric structures having chemically equivalent terminal $\mathrm{P(SiPh_3)_2}$ ligands. By comparison to the spectra for the corresponding $\mathrm{\{M[P(SiMe_3)_2]_2\}_2}$ dimers,[2] at least two resonances would have been expected for polynuclear structures having both bridging *and* terminal ligands. Monomeric solution-phase structures for $\mathrm{Cd[P(SiPh_3)_2]_2}$ and $\mathrm{Sn[P(SiPh_3)_2]_2}$ were also supported by integration of the ^{111}Cd–^{113}Cd and ^{117}Sn–^{119}Sn satellites, respectively, in the ^{31}P NMR spectra. The satellite intensities in both cases established that the $\mathrm{P(SiPh_3)_2}$ groups were terminal ligands, as expected for monomers. We conclude that each of the $\mathrm{M[P(SiPh_3)_2]_2}$ compounds was monomeric in solution. Presumably, two-coordinate linear geometries were adopted, except for $\mathrm{Sn[P(SiPh_3)_2]_2}$, which was required to have a bent geometry by its diamagnetism.[8]

The structure of $\mathrm{Cd[P(SiPh_3)_2]_2}$ in the solid state was determined by X-ray crystallography. Views of the molecule are shown in Figures 1 and 2; selected bond distances and angles are given in the Figure 1 caption. Crystallographic data and atomic positional parameters are given in Tables 1 and 2, respectively. As shown in Figure 1, the molecule exhibited the expected linear, two-coordinate geometry. The cadmium atom resided on a crystallographically imposed center of inversion. The $\mathrm{P(SiPh_3)_2}$ ligands adopted distinctly pyramidal geometries as indicated by the sum of the bond angles about P ($\sum$P = 306.8(3)°). As a requirement of the inversion center, the $\mathrm{P(SiPh_3)_2}$ ligands were arranged in a mutually anti geometry across the metal center, which appears to be a steric minimum. Notable were the very small Si–P–Si angle of 107.7(1)° and the Cd–P distance of 2.427(1) Å, which compared closely to the Cd–P separation of 2.459(1) Å for the terminal $\mathrm{P(SiMe_3)_2}$ ligand in $\mathrm{\{Cd[P(SiMe_3)_2]_2\}_2}$.[2] These structural features will be analyzed below (see Discussion).

Lewis Acidity. The sensitivity of the ^{31}P NMR chemical shift in $\mathrm{Cd[P(SiPh_3)_2]_2}$ to the cadmium coordination environment allowed the determination of formation constants for two $\mathrm{Cd[P(SiPh_3)_2]_2{\cdot}L}$ adducts (L = pyridine and $\mathrm{PMe_3}$). These provide an evaluation of the Lewis aciditity of $\mathrm{Cd[P(SiPh_3)_2]_2}$.

The determinations were prompted by the observation that the ^{31}P NMR chemical shifts of $\mathrm{Cd[P(SiPh_3)_2]_2}$ in toluene and pyridine differed by 52 ppm. The large chemical-shift difference and the donor properties of pyridine suggested the formation of a pyridine adduct $\mathrm{Cd[P(SiPh_3)_2]_2{\cdot}(py)_{\mathit{n}}}$. However, a stable pyridine adduct was *not isolable* from pyridine solutions of $\mathrm{Cd[P(SiPh_3)_2]_2}$, indicating that *if* an adduct formed in solution, then pyridine was only weakly bound.

Further evidence for adduct formation was obtained from NMR titration experiments. When toluene solutions of $\mathrm{Cd[P(SiPh_3)_2]_2}$ were titrated with pyridine, the ^{31}P NMR chemical shift varied smoothly, consistent with the mobile equilibrium in eq 3 under

$$\mathrm{Cd[P(SiPh_3)_2]_2 + L \overset{\mathit{K}_f}{\rightleftharpoons} Cd[P(SiPh_3)_2]_2{\cdot}L} \qquad (3)$$

$$\mathrm{L = pyridine,\ PMe_3}$$

the condition of rapid ligand exchange. A similar result was obtained by titration with $\mathrm{PMe_3}$. One-to-one adduct stoichiometries were assumed, which were supported by the small magnitudes of the formation constants ultimately determined (see below). Formation constants were extracted from the titration data as follows.

The NMR titration experiments were quantitatively analyzed according to the method of Popov and co-workers.[10] Under the condition of rapid ligand exchange on the NMR time scale the chemical shift is given by eq 4, where δ_{obs} is the observed chemical

$$\delta_{\mathrm{obs}} = \delta_f \chi_f + \delta_c \chi_c \qquad (4)$$

shift, δ_f is the chemical shift of free $\mathrm{Cd[P(SiPh_3)_2]_2}$, δ_c is the chemical shift of $\mathrm{Cd[P(SiPh_3)_2]_2{\cdot}L}$, and χ_f and χ_c are the mole fractions of $\mathrm{Cd[P(SiPh_3)_2]_2}$ and $\mathrm{Cd[P(SiPh_3)_2]_2{\cdot}L}$, respectively.

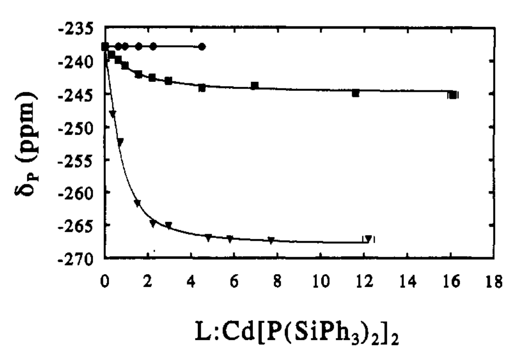

Figure 3. ^{31}P NMR chemical shifts (δ_P) of Cd[P(SiPh$_3$)$_2$]$_2$ in the presence of L, where L = pyridine (▼), PMe$_3$ (■), and THF (●). The data points are the observed shifts, and the curves are the least-squares fits to the data; see text. Note that error bars are assigned to the independent variables (see Experimental Section) and exceed the size of the symbols used for only two of the points.

As derived by Popov and co-workers,[10] an expression for the chemical shift in terms of the equilibrium (formation) constant K_f, the total concentrations of Cd[P(SiPh$_3$)$_2$]$_2$ and L, and δ_f and δ_c was obtained. Least-squares fitting of observed and calculated chemical shifts then yielded the equilibrium (formation) constants.

The data and least-squares fits are plotted in Figure 3 as δ_P vs L:Cd[P(SiPh$_3$)$_2$]$_2$ ratios. The formation constants (K_f's) determined were 1400(150) M^{-1} for L = pyridine and 400(75) M^{-1} for PMe$_3$. As shown in Figure 3, THF did not cause variations in the observed δ_P, suggesting that THF was not an effective Lewis base toward Cd[P(SiPh$_3$)$_2$]$_2$. However, the possibility that Cd[P(SiPh$_3$)$_2$]$_2$ and Cd[P(SiPh$_3$)$_2$]$_2$·THF possessed identical ^{31}P NMR shifts could not be excluded. Similarly, the ^{31}P NMR shifts of Sn[P(SiPh$_3$)$_2$]$_2$ were not observed to vary with added pyridine, PMe$_3$, or THF suggesting but not requiring that Sn[P(SiPh$_3$)$_2$]$_2$ was a weaker Lewis acid than Cd[P(SiPh$_3$)$_2$]$_2$. While ^{119}Sn NMR was a potential alternative to ^{31}P NMR for probing the hypothetical Sn[P(SiPh$_3$)$_2$]$_2$ + L $\rightleftarrows$ Sn[P(SiPh$_3$)$_2$]$_2$·L equilibrium, the ^{119}Sn resonance of Sn[P(SiPh$_3$)$_2$]$_2$ could not be located. Hg[P(SiPh$_3$)$_2$]$_2$ exhibited the same ^{31}P NMR shift in toluene and pyridine (see Experimental Section), suggesting but not requiring that Hg[P(SiPh$_3$)$_2$]$_2$ was also a weaker Lewis acid than Cd[P(SiPh$_3$)$_2$]$_2$. Analogously to Cd[P(SiPh$_3$)$_2$]$_2$, the ^{31}P NMR shifts of Zn[P(SiPh$_3$)$_2$]$_2$ in benzene and pyridine differed by 53 ppm suggesting adduct formation and comparable Lewis-acid behavior. However, the ^{31}P NMR spectrum of Zn[P(SiPh$_3$)$_2$]$_2$ in pyridine was complicated by unassigned minor resonances and a detailed analysis of the Lewis acidity of Zn[P(SiPh$_3$)$_2$]$_2$ was not pursued. Therefore, the successful NMR titration experiments indicated that Cd[P(SiPh$_3$)$_2$]$_2$ was a stronger Lewis acid toward pyridine than toward PMe$_3$, but the magnitudes of the determined formation constants confirmed that the Cd[P(SiPh$_3$)$_2$]$_2$·L adducts had low stabilities.

Discussion

The major focus here has been a comparison of the new M[P(SiPh$_3$)$_2$]$_2$ complexes to the previously known M[N(SiMe$_3$)$_2$]$_2$[1] and {M[P(SiMe$_3$)$_2$]$_2$}$_2$[2] analogs. The discussion below summarizes the close similarities between the properties of M[P(SiPh$_3$)$_2$]$_2$ complexes and their M[N(SiMe$_3$)$_2$]$_2$ analogs that have emerged from comparisons of stabilities, structures, and Lewis acidities. Our results show that the P(SiPh$_3$)$_2$ ligand mimics the N(SiMe$_3$)$_2$ ligand and support the conclusion that the two ligands are effective steric equivalents. Because of the differing properties of the elements N and P outlined below, significantly bulkier silyl substituents on P(SiR$_3$)$_2$ ligands are required to reproduce the classic behavior of the N(SiMe$_3$)$_2$ ligand.

Both the M[P(SiPh$_3$)$_2$]$_2$ and M[N(SiMe$_3$)$_2$]$_2$ families of compounds are thermally robust. The M[N(SiMe$_3$)$_2$]$_2$ compounds are typically distillable liquids or sublimable solids.[1] The M[P(SiPh$_3$)$_2$]$_2$ analogs are solids that possess a similar degree of thermal stability but are apparently too heavy to sublime. In contrast, {M[P(SiMe$_3$)$_2$]$_2$}$_2$ complexes undergo thermal decomposition readily by SiMe$_3$ transfer reactions, giving P(SiMe$_3$)$_3$, and by reductive eliminations, giving (Me$_3$Si)$_2$PP(SiMe$_3$)$_2$.[2] Thermal stability is one of the characteristic features of M[N(SiMe$_3$)$_2$]$_2$ compounds; it is shared by M[P(SiPh$_3$)$_2$]$_2$ compounds but not {M[P(SiMe$_3$)$_2$]$_2$}$_2$ compounds.

Both the M[P(SiPh$_3$)$_2$]$_2$ and M[N(SiMe$_3$)$_2$]$_2$ families of compounds exhibit monomeric, two-coordinate structures. Because M[N(SiMe$_3$)$_2$]$_2$ compounds are volatile, their structures have been determined by gas-phase electron diffraction in several cases, including M = Zn,[14] Cd,[15] Hg,[16] and Sn.[17] The first three examples cited are linear in the gas phase, whereas the last is bent. The X-ray crystal structure[17] of Sn[N(SiMe$_3$)$_2$]$_2$ shows that it has the same structure in the solid state as in the gas phase. To our knowledge two solid-state X-ray crystal structures of bulkier silyamido complexes have been reported, Zn[N(SiMe$_3$)(*t*-Bu)]$_2$[18] and Zn[N(SiMePh$_2$)$_2$]$_2$,[19] both of which are two-coordinate, linear monomers. The molecular structure of Cd[P(SiPh$_3$)$_2$]$_2$ in Figure 1 confirms that it is also is a two-coordinate, linear monomer. To our knowledge Cd[P(SiPh$_3$)$_2$]$_2$ is the first two-coordinate cadmium compound for which a solid-state X-ray crystal structure has been determined. In other cases, monomeric structures of M[N(SiMe$_3$)$_2$]$_2$ and M[P(SiPh$_3$)$_2$]$_2$ compounds have been demonstrated cryoscopically or spectroscopically. The ability to stabilize low-coordinate metal environments is a classic feature of the N(SiMe$_3$)$_2$ ligand, and it is shared by the P(SiPh$_3$)$_2$ ligand.

In contrast, {M[P(SiMe$_3$)$_2$]$_2$}$_2$ compounds exhibit dimeric, three-coordinate structures (see **I**) as a result of the intrinsically stronger bridging tendencies of PR$_2$ ligands compared to NR$_2$ ligands.[2] The stronger bridging tendencies are due to the larger size and lower electronegativity of P compared to N and to the pyramidality of terminal P(SiR$_3$)$_2$ ligands as compared to the planarity of terminal N(SiR$_3$)$_2$ ligands resulting from the isovalent hybridization ability of N.[2] These effects combine to support higher coordination numbers about P than N or, in other words, to produce considerably less-hindered coordination environments about P. Terminal PR$_2$ ligands are therefore much more likely to increase the coordination number about the pnictide (P, N) element by adopting bridging positions.

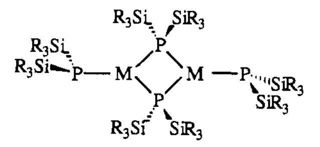

I

The inherently less-hindered environments about the P atoms in phosphido ligands as compared to the N atoms in amido ligands are nicely revealed by comparing the structural features of N(SiPh$_3$)$_2$ groups to the P(SiPh$_3$)$_2$ group in Cd[P(SiPh$_3$)$_2$]$_2$. Power and co-workers recently reported the structures of (THF)$_2$Li[N(SiPh$_3$)$_2$], in which the N(SiPh$_3$)$_2$ group is a terminal ligand, and [Li(12-crown-4)$_2$][N(SiPh$_3$)$_2$]·THF, in which the N(SiPh$_3$)$_2$ group is a free anion.[20] The Si–N–Si angles in these compounds have the exceptionally large values of 140.5(2) and

---

(14) Haaland, A.; Hedberg, K.; Power, P. P. *Inorg. Chem.* **1984**, *23*, 1972.
(15) Alyea, E. C.; Fisher, K. J.; Fjeldberg, T. *J. Mol. Struct.* **1985**, *127*, 325.
(16) Alyea, E. C.; Fisher, K. J.; Fjeldberg, T. *J. Mol. Struct.* **1985**, *130*, 263.
(17) Fjeldberg, T.; Hope, H.; Lappert, M. F.; Power, P. P.; Thorne, A. J. *J. Chem. Soc., Chem. Commun.* **1983**, 639.
(18) Rees, W. S.; Green, D. M.; Heese, W. *Polyhedron* **1992**, *11*, 1697.
(19) Power, P. P.; Ruhlandt-Senge, K.; Shoner, S. C. *Inorg. Chem.* **1991**, *30*, 5013.
(20) Chen, H.; Bartlett, R. A.; Dias, H. V. R.; Olmstead, M. M.; Power, P. P. *J. Am. Chem. Soc.* **1989**, *111*, 4338.

154.9(3)°, respectively, indicating substantial steric interactions between the bulky $SiPh_3$ substituents. In contrast, the Si–P–Si angle in $Cd[P(SiPh_3)_2]_2$ has the small value of 107.7(1)°, indicating the *lack* of substantial steric interactions between the bulky $SiPh_3$ substituents in the distinctly pyramidal $P(SiPh_3)_2$ ligand. The normal Cd–P separation exhibited by $Cd[P(SiPh_3)_2]_2$ (see Results) contrasts markedly with the exceptionally long Li–N separation in $[Li(12\text{-crown-}4)_2][N(SiPh_3)_2]\cdot THF$, which reflects complete dissociation of the Li–N interaction.[20] Clearly, the steric environment about N in $N(SiPh_3)_2$ is significantly more hindered than the environment about P in $P(SiPh_3)_2$. To compensate for this natural difference and to defeat the bridging tendencies, phosphido ligands must possess considerably bulkier substituents to have properties similar to amido ligands.

Finally, $M[P(SiPh_3)_2]_2$ and $M[N(SiMe_3)_2]_2$ compounds exhibit similar Lewis acidities. Very few adducts of the type $M[N(SiMe_3)_2]_2\cdot L$ have been reported, consistent with the ability of the $N(SiMe_3)_2$ ligand to stabilize low-coordinate metal centers. The crystalline one-to-one adducts $Zn[N(SiMe_3)_2]_2\cdot py$ and $Zn[N(SiMe_3)_2]_2\cdot 4\text{-Mepy}$ have been isolated;[21] these are the only examples we know of involving $N(SiMe_3)_2$ analogs of the $P(SiPh_3)_2$ complexes discussed herein. We have found that pyridine and PMe_3 coordinate weakly and reversibly to $Cd[P(SiPh_3)_2]_2$, with ΔG values of only −4.3(1) and −3.5(1) kcal/mol, respectively. Despite the low coordination numbers for the metal atoms in $M[P(SiPh_3)_2]_2$ and $M[N(SiMe_3)_2]_2$ compounds, the similarly bulky $P(SiPh_3)_2$ and $N(SiMe_3)_2$ ligands discourage the coordination of additional ligands, thus providing $M[P(SiPh_3)_2]_2$ and $M[N(SiMe_3)_2]_2$ compounds with similarly weak Lewis acidities.

In summary, $M[P(SiPh_3)_2]_2$ and $M[N(SiMe_3)_2]_2$ compounds exhibit closely similar properties as a result of the effective steric equivalency of the $P(SiPh_3)_2$ and $N(SiMe_3)_2$ ligands. The bulkier substituents at P are required to defeat the naturally greater bridging tendencies of phosphido ligands.

Acknowledgment. Funding was provided by the Petroleum Research Fund, administered by the American Chemical Society, and an NSF Presidential Young Investigator award, supported by the Monsanto Co. and the Eastman Kodak Co. Washington University's X-ray Crystallography Facility was funded by the NSF Chemical Instrumentation Program (Grant CHE-8811456). The Washington University High-Resolution NMR Service Facility was funded in part by NIH Biomedical Research-Support-Shared-Instrument Grant 1 S10 RR02004 and a gift from the Monsanto Co.

Supplementary Material Available: Tables listing details of the crystallographic data collection, bond distances, bond angles, calculated hydrogen atom parameters, and anisotropic thermal parameters (7 pages). Ordering information is given on any current masthead page.

---

(21) Fisher, K. J. *Inorg. Nucl. Chem. Lett.* **1973**, *9*, 921.